Revista Facultad de Ingeniería

Title: **Methodology for forecasting precipitation related to El Niño when historical meteorological data are incomplete**

Authors: María Felicia Jiménez-Lavie, Cecilia Martín-del-Campo, José Luis Lezama-Campos Edgar Gerardo Mendoza-Baldwin and Rodolfo Silva-Casarín

DOI: **10.17533/udea.redin.20241250**

To appear in: *Revista Facultad de Ingeniería Universidad de Antioquia*

Received: September 07, 2023
Accepted: December 03, 2024
Available Online: December 09, 2024

when historical meteorological data are incomplete, *Revista Facultad de Ingeniería Universidad de Antioquia*. [Online]. Available: https://www.doi.org/10.17533/udea.redin.20241250

Methodology for forecasting precipitation related to El Niño when historical meteorological data are incomplete

Metodología para pronosticar la precipitación de El Niño cuando los datos meteorológicos históricos son incompletos

María Felicia Jiménez-Lavie[1] https://orcid.org/0009-0003-3240-2338, Cecilia Martín- del-Campo[1] https://orcid.org/0000-0002-6173-7546 José Luis Lezama-Campos[2] https://orcid.org/0000-0003-4142-5876 Edgar Gerardo Mendoza-Baldwin[3] https://orcid.org/0000-0002-1991-4721 Rodolfo Silva-Casarín[3*] https://orcid.org/0000-0003-0064-9558

[1]Facultad de Ingeniería, Universidad Nacional Autónoma de México. Edificio Bernardo Quintana, Piso 1, C.U, Coyoacán. C. P 04510. Coyoacán, México.

[2]Instituto de Geología, Universidad Nacional Autónoma de México. Circuito Interior s/n, Coyoacán. C. P. 04510. Coyoacán, México.

[3]Instituto de Ingeniería, Universidad Nacional Autónoma de México. Circuito Escolar Ingeniería S/N, C.U., Coyoacán. C. P. 04510. Coyoacán, Mexico.

Corresponding author: Rodolfo Silva-Casarín
E-mail: RSilvaC@iingen.unam.mx

KEYWORDS
ENSO phases; seasonal precipitation forecast; rainfall anomaly; precipitation patterns in Mexico; the influence of ENSO
Fases del ENOS; pronósticos de lluvia mensual y estacional; anomalía de precipitación; patrones de precipitación en México; influencia del ENOS

ABSTRACT: The interactions between the ocean and the atmosphere produce various climatic phenomena, such as the El Niño-Southern Oscillation (ENSO), that influence hydrological systems. This study serves as a basis for water resource management and planning in reservoirs and hydroelectric generation, in both the short and long term. A methodology is proposed to study the potential influence of extreme phases of ENSO on the amount of monthly and seasonal precipitation in areas where the weather stations do not have a complete historical data record. A case study is presented of the seasonal precipitation forecast for the largest water reservoir in Mexico. Data from 18 weather stations in the hydrological sub-region Grijalva-La Concordia, in the state of Chiapas, were examined, the highest on the river course of the rainwater catchment dam of the Grijalva Hydroelectric Complex, the most important complex of its kind in Mexico. From the results it is expected that climate change will bring more frequent El Niño phases. The proposed methodology has been validated, making it an effective

tool to evaluate the effects of ENSO on precipitation. The methodology is applicable to other regions, particularly in developing countries where historical information is often incomplete.

RESUMEN: La interacción océano-atmósfera es un proceso que da paso a diferentes fenómenos climáticos que tienen una fuerte influencia en los sistemas hidrológicos, siendo el fenómeno El Niño-Oscilación Sur (ENOS) uno de ellos. En este trabajo se planteó una metodología para el estudio de la influencia de las fases extremos del ENOS sobre la cantidad de precipitación mensual y estacional en regiones donde las estaciones climatológicas no tienen un registro histórico completo de datos. Para ello se tomaron 18 estaciones climatológicas ubicadas en la Subregión Hidrológica Grijalva-La Concordia en Chiapas, México. El estudio de la influencia de los cambios de fase del ENOS en esta región es de suma importancia ya que es donde se encuentra la Presa La Angostura, la cual tiene el mayor embalse de agua en México y es la primera presa de captación pluvial del Complejo Hidroeléctrico Grijalva, el más importante del territorio mexicano. Se espera que el cambio climático acelere los procesos cíclicos de las fases del ENOS, dando lugar a fases de El Niño más frecuentes. Por este motivo, este estudio sirve de base para una gestión y planificación del recurso hídrico en esta zona en el corto y largo plazo. La metodología planteada es una herramienta simple y eficaz, la cual permite evaluar el grado de influencia del ENOS en la precipitación, sin que para ello se tenga una serie completa de datos históricos.

1. Introduction

The relationship between the atmosphere and the ocean has a strong, complex, and non-linear behaviour. The main processes in this interaction are heat exchanges, rainfall, evaporation, and wind shear. Running through all these interactions is a continuous cycle of energy and matter transfer that is vital for the understanding of the different meteorological and climatic processes that take place on Earth [1]. This interaction works as a forcing agent in hydrological systems at different time scales and affects the behaviour of meteorological and hydrographic variables, such as hydrological fluxes, precipitation, and air temperature and humidity [2].

One example of such atmosphere-ocean interaction is the El Niño-Southern Oscillation phenomenon, (ENSO), a natural phenomenon with interannual frequency, characterised by fluctuating ocean surface temperatures in the central and eastern tropical Pacific Ocean [3]. Of all the large-scale ocean-atmospheric modes, ENSO has most impact on the interannual variability of global climate [4], directly affecting most of the precipitation and temperature patterns on the planet [5]. The extreme phases of this phenomenon are El Niño (warm) and La Niña (cool), compared to the Neutral phase [6]. The Oceanic Niño Index (ONI), developed by the National Oceanic and Atmospheric Administration (NOAA), is the primary indicator for monitoring the oceanic part of this climate pattern [7], and measures the condition and phase of ENSO in the Equatorial Pacific [8].

El Niño and La Niña occur on average every 3 to 5 years, although historical records show that their interval of occurrence may be between 2 and 7 years. The approximate duration of each is 9 to 12 months, but some episodes have persisted for as long as 2 years. It should be noted that an El Niño phase is not

always followed by a La Niña phase [6], and that generally, El Niño occurs more frequently than La Niña [9]. While the ENSO cycle has persisted with no major perturbations for the past 11,000 years, scientists forecast disruptions as a consequence of climate change [3]. For example, [10] suggested that El Niño events will be more frequent in the future. [11] are more specific, predicting a 20% increase in the frequency of El Niño occurrence in the 21st century.

The extreme ENSO phases can cause severe storms, droughts, or floods, which may produce secondary outcomes impacting agriculture, public health, freshwater availability, energy generation, and economic activity in various regions of the world [12 and 13]. Fish production can also be affected, as changes in ocean temperatures and currents occurring during El Niño impact marine life [13]. These effects do not occur evenly across the world. For example, the probability of drought increases in India, Indonesia, Australia and much of the Amazon during El Niño, while the south of the USA tends to have more precipitation. During La Niña, this pattern is reversed, with wetter conditions for Indonesia, Australia and parts of the Amazon, and drier conditions in the south of the USA [12]. El Niño and La Niña can even affect the same country differently. For example, from autumn to spring, El Niño generally causes increased precipitation and sometimes destructive flooding in the southern United States. In contrast, La Niña generally causes drier weather in the south and cooler and wetter weather in the northwest [13].

Although a considerable number of reports exist on changes in water availability due to the ENSO cycle, in Mexico, no planning or policies for water management take this into consideration. Arguably, the reason is the lack of detail in forecasting local consequences. This work analyses the effects of the extreme phases of ENSO on monthly mean precipitation patterns in the La Concordia Hydrological Sub-Region (HSR) in Chiapas, Mexico. This HSR was selected as it hosts Mexico's most important hydroelectric system. We used the historical records of 18 weather stations located in the HSR, which are operated by the National Water Commission (CONAGUA) and the Ministry of Environment and Natural Resources (SEMARNAT). Although these weather stations were carefully selected based on the quality and quantity of available data, their data series are incomplete and historical records do not always have an exact temporal coincidence between the stations. It was, therefore, necessary to apply a methodology that would fit the available data and allow us to characterise the ENSO-related hydrology in the study area.

Most works that analyse the influence of ENSO on rainfall patterns use the historical records of weather stations in the areas studied. Incomplete or non-existent historical data is a common problem, particularly in developing countries, and makes it impossible to use conventional statistical methods in such research. For this reason, we propose a methodology where the stations are characterised by their historical records during ENSO phases, which give more realistic values than simple historical averages. The main goal is to achieve a better forecast of the rainfall regime related to ENSO extreme phases.

The paper is organised as follows: the information for the study area collected is analysed and the methodology used is described. The results are then given, analysed, and validated. Finally, the conclusions are presented.

2. Methodology

2.1. Study Area

In Mexico, climate variability is often associated with the ENSO phenomenon [14]. El Niño has asymmetric effects across the country, with higher rainfall in the north and dry periods in the centre and south during the summer. In winter, a positive ENSO phase causes a precipitation anomaly in the north, while findings on its effects in the south and centre remain divergent [15].

The Hydrological Regions (HR) in southeast Mexico contain two-thirds of the country´s available water [16]. Hence, it is important to anticipate the effects of the extreme phases of ENSO on the hydro-meteorological conditions here. With knowledge of these variabilities, strategic measures can be established to manage the water resources affected by any increase in the occurrence or intensity of El Niño. The basins in the HRs of south-eastern Mexico are important, socioeconomically, and environmentally, and are highly vulnerable. The La Concordia HSR was selected for this study as it is the most important in the country.

HR 30 is one of the wettest HRs in Mexico [17] and is home to the biggest rivers in the country: the Usumacinta and the Grijalva [18]. It covers 91,345 km^2, and its ecosystems host 64% of the known national biodiversity, as shown in Figure 1. The country's four most important hydroelectric plants are found in this HR, forming the Grijalva Hydroelectric Complex [19], which generates 38.2% of the country´s installed hydroelectric capacity [20].

The HSR La Concordia is part of this HR, and is comprised of twelve hydrographic basins, as seen in Figure 2. The flow in the hydrological basin of the Lagartero River continues to the Selegua River basin, and those of the Yayahuita, Zacualpa and Papizaca contribute their flow to the San Miguel River basin. The La Concordia, Selegua, San Miguel, Aguacatenco, Aguzarca, San Pedro and Grande (or Salinas), hydrological basins contribute their flow to the La Angostura Dam basin and this contributes to the Chicoasén Dam Hydrological Basin [19].

The main river in this HSR is the Grijalva, which rises in the Republic of Guatemala and flows into the Gulf of Mexico. The region lies between the border with Guatemala and the La Angostura dam [21], covering approximately 9,644 km^2. The rainy season here occurs typically from May to October [19], and the Angostura Dam is the largest rain-fed dam of the Grijalva hydroelectric system (see Figure 3). The hydroelectric plant at the dam has an installed electricity generation capacity of 900 MW [22], which is 7.2 % of the installed hydroelectric capacity in Mexico [20]. The dam is also the largest reservoir in the country, with a capacity at the Maximum Ordinary Water Level of 12762 hm^3 [23]. The main uses of this water include electricity generation, flood control, fishing, and aquaculture exploitation [24].

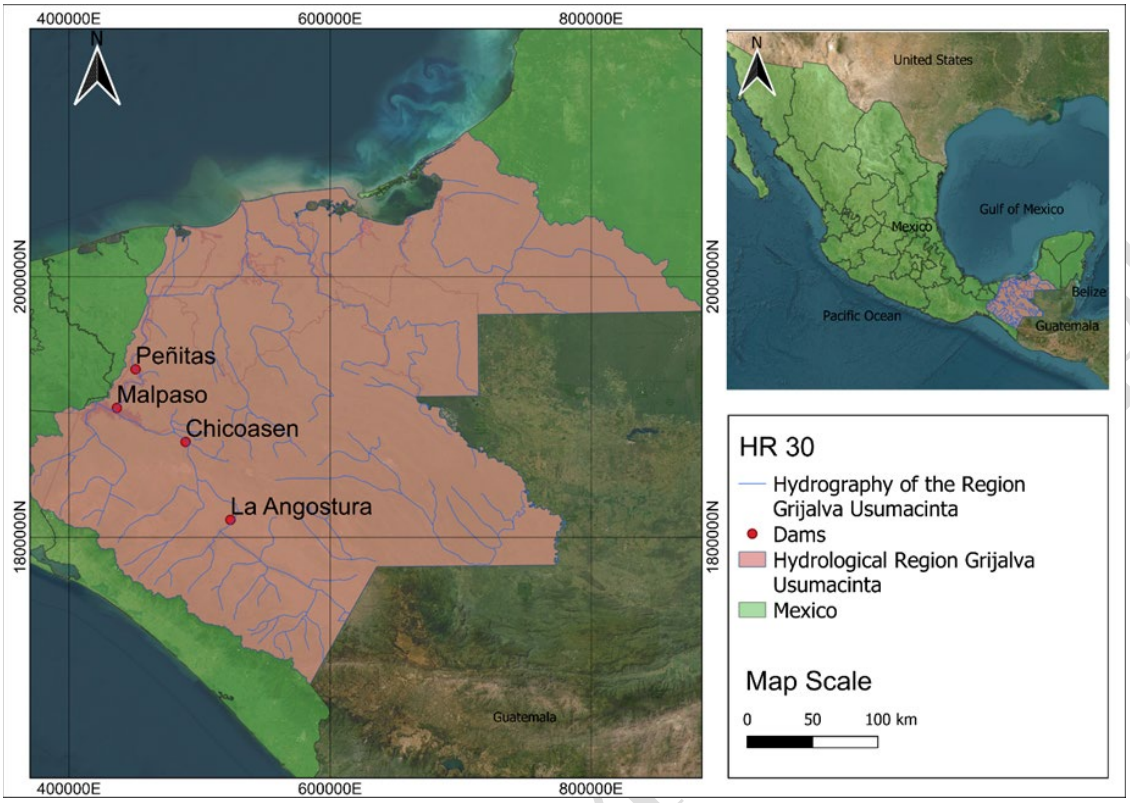

Figure 1 Location of HR 30 Grijalva-Usumacinta (The map reference system is UTM Zone 15 N, QGIS Desktop 3.18.2 and CONABIO Geoportal database)

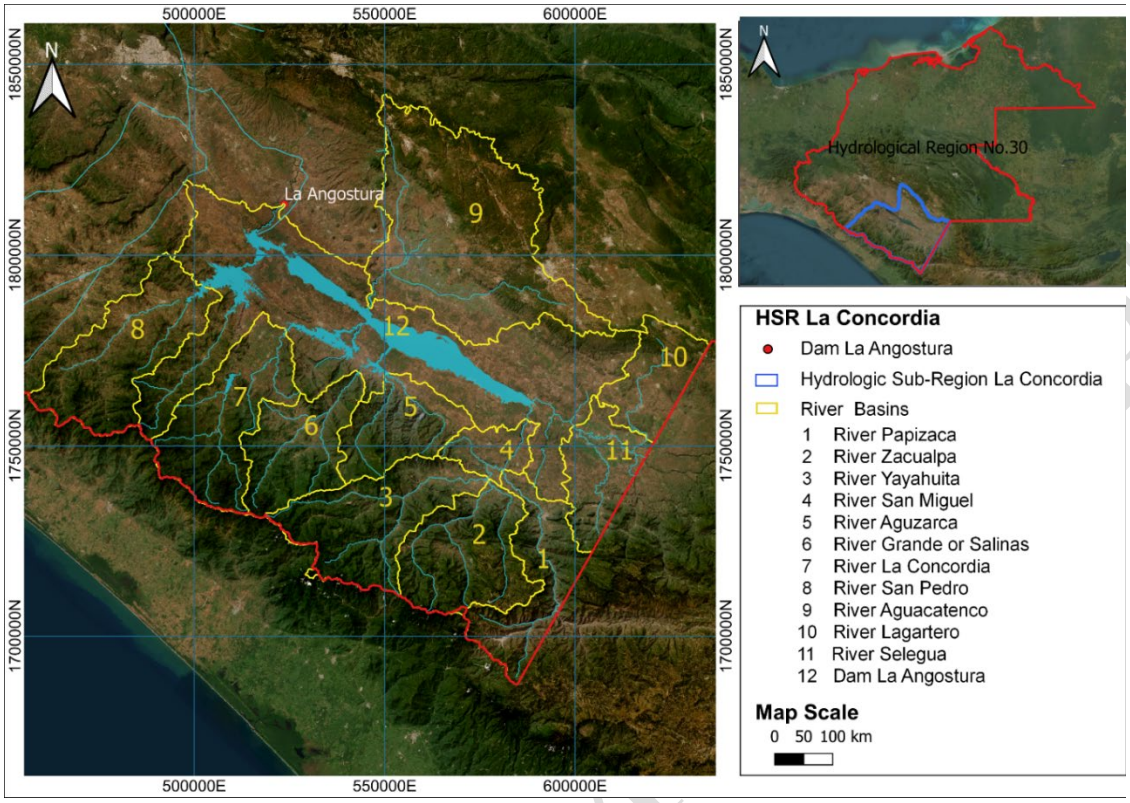

Figure 2 Location of the La Concordia HSR and the river basins within it (The map reference system is UTM Zone 15 N, QGIS Desktop 3.18.2 and CONABIO Geo portal database)

2.2. Analysis of the information

For the analysis of the historical precipitation data [25], eighteen stations from the weather stations network were selected according to the following criteria:

- Presently operational.
- Historical data record of 30 years or more (Table 1).
- The historical record was at least 85% complete (Table 1).
- The final group was distributed across the HSR as evenly as possible.

Table 1 shows the list of weather stations selected for the analysis in the La Concordia HSR.

Table 1 Data of the weather stations studied

		Location			Data			
Station	**Name**	**Altitude (masl)**	**Latitude (°)**	**Longitude (°)**	**Home (year)**	**Final (year)**	**Total (years)**	**Missing data (%)**
7002	Abelardo L. Rodríguez	1920	16.3792	-92.2375	1963	2017	55	3.00
7007	Amatenango del Valle	1820	16.5281	-92.4378	1964	2016	53	2.13
7009	Aquespala	617	15.7942	-91.9203	1957	2013	57	4.98

7021	Catarinitas	945	15.9025	-92.4828	1985	2014	30	6.49
7025	Comitan (OBS)	1709	16.2333	-92.1333	1982	2018	37	8.33
7037	Finca Cuxtepeques	1550	15.7286	-92.9689	1951	2015	65	9.30
7054	Finca A. Prusia	1040	15.7319	-92.7942	1954	2012	59	14.45
7067	Frontera Amatenango	900	15.4336	-92.1142	1970	2017	48	13.85
7070	Guadalupe Grijalva	630	15.6936	-92.1611	1961	2015	55	6.07
7094	La Mesilla	1210	16.1842	-92.2875	1971	2016	46	7.39
7119	Motozintla (SMN)	1260	15.3642	-92.2481	1950	2018	69	5.27
7145	San Francisco	540	15.8708	-92.9536	1950	2017	68	7.60
7180	Jaltenango (CFE)	640	15.8708	-92.7239	1970	2016	47	2.84
7205	Comitán (DGE)	1630	16.2511	-92.1342	1961	2016	56	1.63
7224	Chicomuselo	550	15.752	-92.274	1975	2017	43	8.98
7236	Revolución Mexicana	540	16.163	-93.076	1977	2017	41	7.80
7329	Cascajal	650	16.309	-92.486	1980	2018	39	6.02
7342	Benito Juárez	580	16.0828	-92.8406	1980	2017	38	13.08

Figure 3 Location of the weather stations studied (The map reference system is UTM Zone 15 N, QGIS Desktop 3.18.2 and CONAGUA database)

An exploratory analysis of the data from each of the weather stations in Table 1 revealed significant porosity in the records. To complete the missing daily precipitation data, we intended to use the U.S. Weather Bureau method and a linear regression method. However, these methods require the daily precipitation records from at least four other stations, as close as possible and uniformly located around the incomplete station [26]. For the La Concordia stations, none fulfilled the methods' requirements, so they were not applicable.

The solution found was extracting the daily-monthly precipitation data for each station, according to El Niño, La Niña and Neutral episodes, using the ONI database from 1950 to the present, available on the NOAA website, [27]. Although the magnitude and duration of each El Niño and La Niña episode are different [28] and there have been some unusually strong El Niño and La Niña episodes [29], it was assumed that their influence on precipitation in the study area was similar during each episode.

2.3. Analysis of the information

For each weather station, the following procedure was followed:

- The daily precipitation data for each month was separated from the recorded measurements for each year, using the ONI data published on the NOAA website, [27], and annotating whether the month was Niño, Niña or Neutral.

- From this monthly data, the mean (historical), median, mode, standard deviation and variance were found for each month.
- The probability of monthly rainfall according to the ENSO phase was found using Equation 1:

$$\mathrm{P}_r(x) = \frac{N_r(x)}{N_T(x)} \tag{1}$$

where:

$\mathrm{P}_r(x)$: rainfall probability in the month X

$N_r(x)$: number of data with rainfall recorded in the month X

$N_T(x)$: number of data recorded in total in the month X

X: month of the year

- In a similar way, the average monthly precipitation (Total) was found for each station, according to the ENSO phase, using Equations 2 and 3:

$$d_r(x) = \mathrm{P}_r(x) \times d_m(x) \tag{2}$$

$$R_m(x) = d_r(x) \times R_h(x) \tag{3}$$

where:

$d_r(x)$: days with rainfall in the month X.

$\mathrm{P}_r(x)$: rainfall probability in the month X.

$d_m(x)$: numbers of days in the month X.

$R_m(x)$: monthly average rainfall calculated in the month X.

$R_h(x)$: historical average rainfall in the month X.

X: month of the year.

- The rainfall anomaly was then calculated according to [30], for the extreme ENSO phases using Equation 4:

$$A_r(x) = \left(\frac{R_{m.ENSO}(x) - R_{m.Normal}(x)}{R_{m.Normal}(x)} \right) \tag{4}$$

where:

$A_r(x)$: anomaly of the rainfall in the month X.

$R_{m.ENSO}(x)$: monthly rainfall calculated according to the Extrema ENSO phase (El Niño or La Niña), using Equation 3.

$R_{m.Normal}(x)$: monthly rainfall calculated according to the Normal ENSO phase for month x, using Equation 3.

X: month of the year.

Once this information was collected and processed for all the weather stations in Table 1, the following methods were used to calculate each of the parameters to find the volume total monthly precipitation in the region.

- The Thiessen Polygon Method [31] was used to find the area of influence of each weather station in the study area [32]. The size and shape of these areas of influence depend on the distribution of the stations [33]. Disadvantages of this method are that it does not consider the influence of the topography of the study area [31], and that the associated error cannot be estimated, since the value for each polygon is obtained from a single point [33]. Therefore, two calculation methods were used in this study. To calculate the Thiessen Polygons, we used the computer program QGIS Desktop, version 3.18.2. The resulting areas of influence of each station are shown in Figure 4. Then, Equation 5 was used to calculate average monthly precipitation in the La Concordia HSR according to the ENSO phase.

$$R_{T.HSR}(x) = \sum_{i=1}^{18} \left(R_{m,i}(x) \times A_I \right) \tag{5}$$

where:

i: stations studied (in total 18).

$R_{T.HSR}(x)$: monthly average rainfall volume total calculated in the La Concordia HSR for The Thiessen Polygon Method.

$R_{m,i}(x)$: Monthly average rainfall calculated using equation 3 for the station i.

A_I: Influence area for the station i.

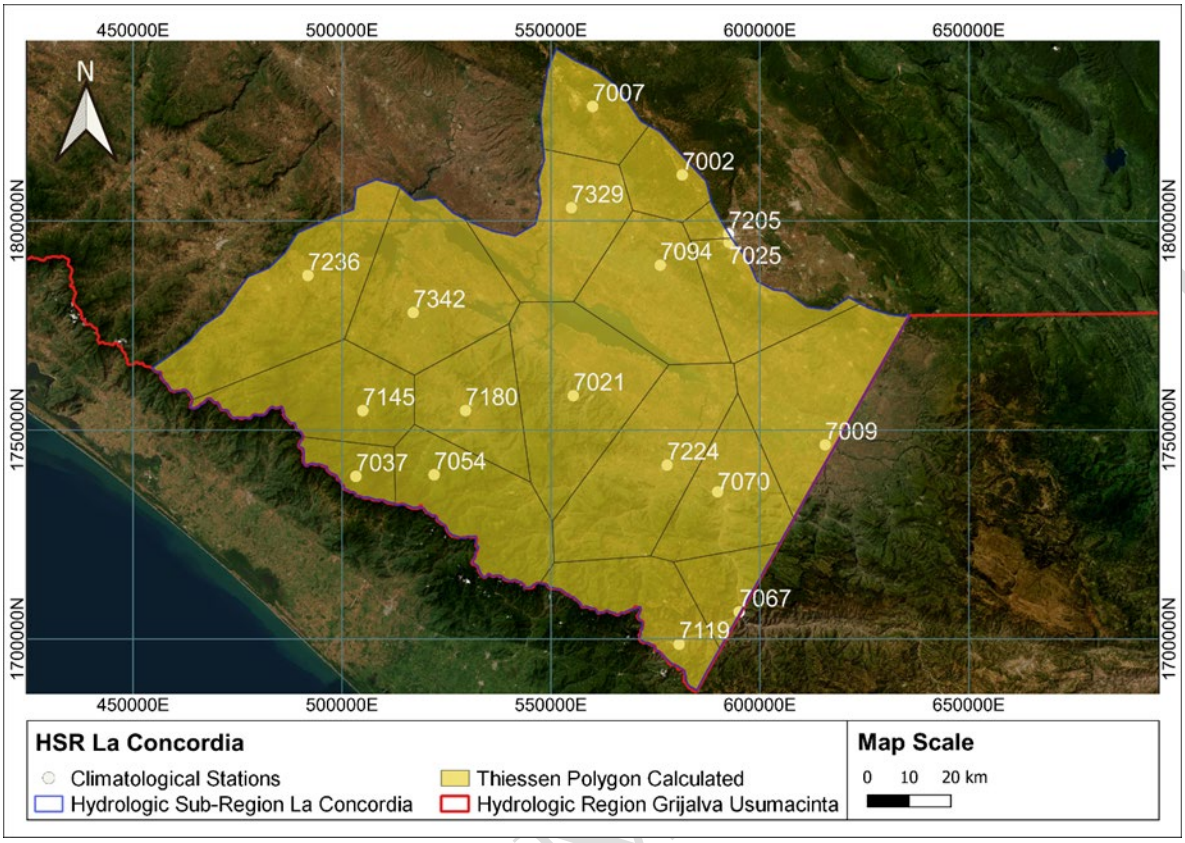

Figure 4 Location of the weather stations studied (The map reference system is UTM Zone 15 N, QGIS Desktop 3.18.2 and CONAGUA database)

- The Kriging spatial interference method was used to obtain a series of continuous data for all the stations based on the distance between the points with and without data [32]. To make these calculations, MATLAB R2019a was used. The resulting square matrix of 18X18 equal area sectors gave values calculated from the initial data. Then, according to the ENSO phase, to calculate the monthly precipitation, Equation 6 was used. The only drawback found in the application of this method was that we could not adjust the precipitation calculation to the exact area of the La Concordia HSR.

$$R_{K.HSR}(x) = A_S \times \sum_{j=1}^{324} \left(R_{m,j}(x) \right) \tag{6}$$

where:

j : number of elements in the 18 x 18 matrix (324).

A_S: area of each sector of the 18x18 matrix.

$R_{K.HSR}(x)$: monthly average rainfall volume total calculated in the La Concordia HSR for the Kriging spatial interference method.

$R_{m,j}(x)$: monthly average rainfall calculated for the Kriging spatial interference method for each element of the 18x18 matrix.

2.4. Validation of the Methodology

To test the proposed methodology for missing data estimation, a period of approximately 20 years (November 1963 to April 1984) was analysed for station 7009, which shows a complete record of precipitation data. The proposed methodology was applied, and the analysed rainfall period was reconstructed from the results obtained with 100% of the data. Then, 0.5, 1.0, 2.5, 5.0, 5.0, 7.5, 10.0, 12.5, 15.0, 20.0, 25.0, 30.0 and 40.0% of data were randomly removed and computed. Figure 5 shows a comparison of the original and estimated data.

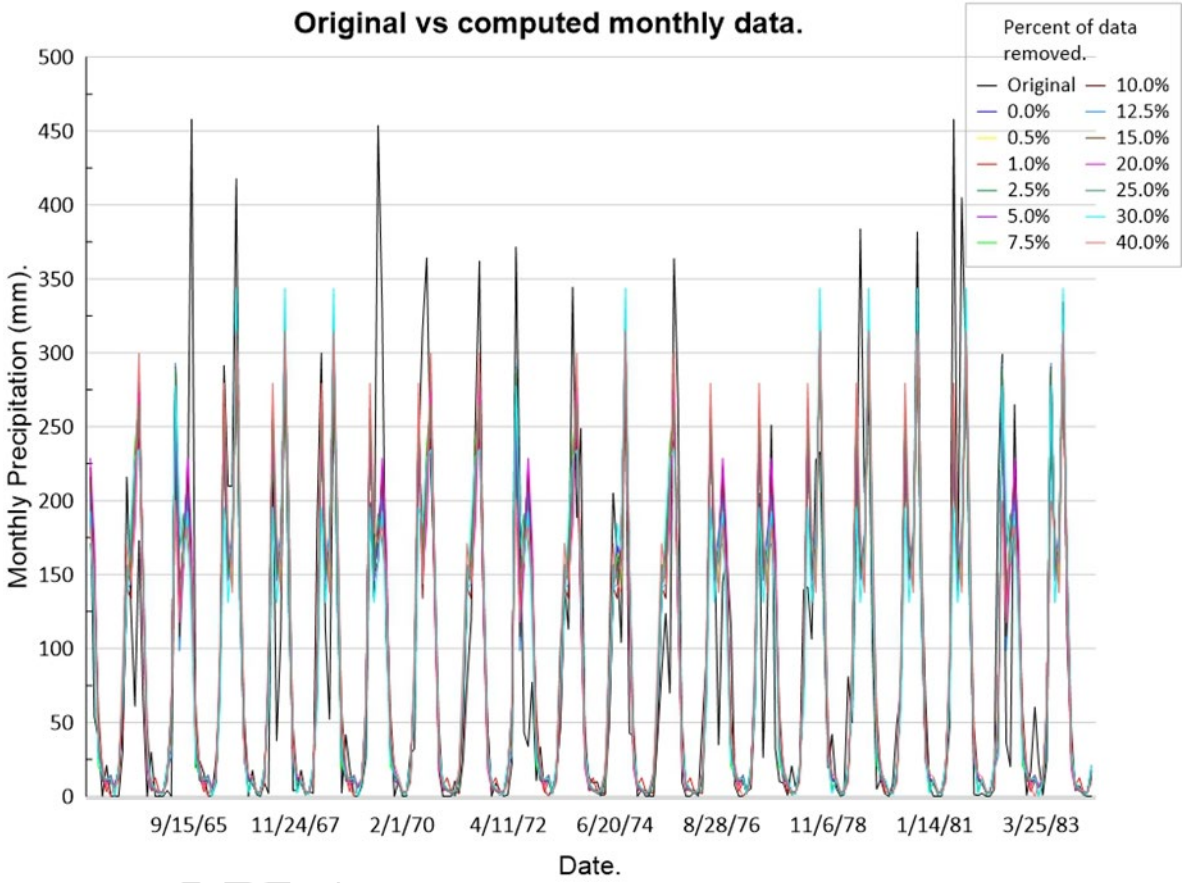

Figure 5 Comparison of monthly precipitation of station 7009 and monthly precipitation reconstructed using the methodology proposed

For all the time series that were reconstructed with the proposed methodology, the correlation with the original series was over 82.2%. When comparing the reconstructed series with different amounts of data removed, the mean absolute percentage error (MAPE) yielded an average value of 30.66% with a standard deviation of 2.03. This MAPE value obtained is considered a reasonable forecast [34]. While for the dry months, a mean MAPE value is 52.96% with a standard deviation of 2.85, which is considered inaccurate [34], as seen in Table 2. The MAPE was calculated using Equation 7. In Table 2, it can be seen that the MAPE values increase as the percentage of data removed increases, although this increase is not directly proportional. The results show that the methodology adequately reconstructs the average monthly precipitation.

However, it does not fit the extreme values well, which causes the errors to increase in the rainy months. In the dry months, the precipitation values are so low that a very small variation produces very large errors.

$$MAPE = 100 \times \left(\frac{1}{n} \sum_{i=1}^{n} \frac{\left| A_i - F_i \right|}{A_i} \right) \tag{7}$$

where:

A_i: current value.

F_i: predicted value.

n: total number of observations.

Table 2 Monthly MAPE values for the different time series reconstructed, using the proposed methodology

Percent of data removed from the original series (%)	**Monthly MAPE values (%)**	
	Dry months	**Rainy months**
0	49.74	29.06
0.50	50.15	29.68
1.00	50.21	29.73
2.50	50.27	29.74
5.00	50.83	29.76
5.50	51.71	29.81
10.00	52.56	30.05
12.50	53.09	30.25
15.00	54.63	30.43
20.00	55.37	30.61
25.00	55.94	30.74
30.00	56.93	32.52
40.00	57.95	36.86

When using the proposed methodology to determine the mean precipitation, Equations 8 and 9 during the rainy and/or dry periods, the results are very close to the real values for the time periods with the total data, or with some of the missing data. The mean MAPE value for the rainy months is 12.77% with a standard deviation of 0.83 (Table 3), which is considered a good forecast. For the dry season, the mean MAPE value is 30.37% with a standard deviation of 3.03, considered a reasonable forecast [34].

$$P_{D.S} = R_{Nov} + R_{Dec} + R_{Jan} + R_{Feb} + R_{Mar} + R_{Apr} \tag{8}$$

$$P_{R.S} = R_{May} + R_{Jun} + R_{Jul} + R_{Aug} + R_{Sep} + R_{Oct} \tag{9}$$

Where:

$P_{D.S}$: total rainfall in the dry season.

$P_{R.S}$: total rainfall in the rainy season.

R_{Jan}, R_{Feb}, ..., R_{Dec}: monthly rainfall values, these were calculated using the proposed methodology (Equation 4). It is worth mentioning that the ENSO phase was considered when adding the monthly precipitation values of Equations 8 and 9.

Figure 6 shows the rainfall during various rainy and dry seasons, between November 1963 and April 1984. The original data series, and those reconstructed with the methodology proposed, at 100%, 99.5%, 99.0%, 97.5%, 95.0%, 92.5%, 90.0%, 87.5%, 85.0%, 80.0%, 75.0%, 70.0% and 60.0% of the data, respectively.

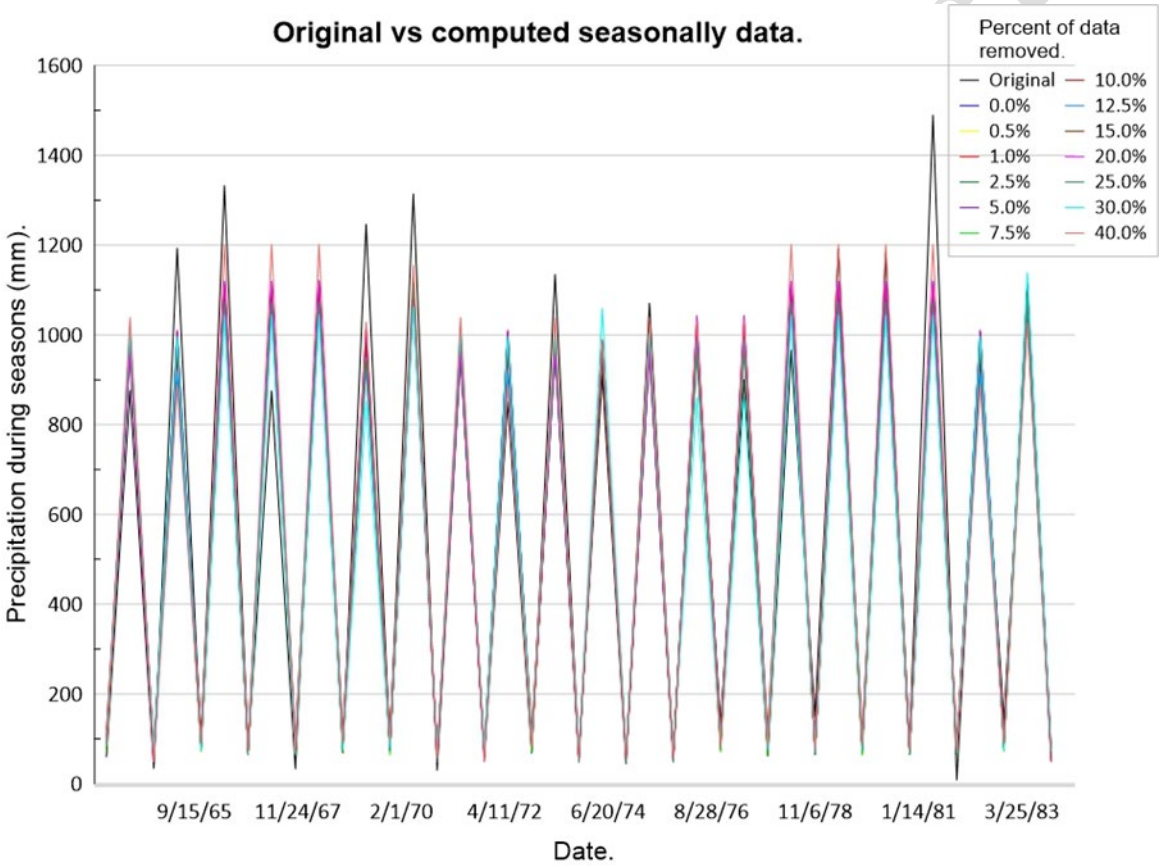

Figure 6 Comparison of the real seasonal precipitation of station 7009 with the seasonal precipitation reconstructed with the methodology proposed for periods with different amounts of data (compared to the original series)

Table 3 MAPE values for the different time series reconstructed by using the proposed methodology

Percentage of data removed from the original series (%).	**MAPE values for precipitation periods (%).**	
	Dry	**Rainy**
0	27.70	11.88

0.50	27.66	11.93
1.00	30.20	11.94
2.50	28.40	12.10
5.00	28.41	12.56
5.50	27.92	12.66
10.00	29.78	12.69
12.50	30.64	12.88
15.00	30.27	12.95
20.00	30.48	12.97
25.00	31.85	13.01
30.00	35.71	13.82
40.00%	37.51	14.87

It is seen that the data source used in the application of the methodology must be reliable and the data must be validated as thoroughly as possible. Techniques such as the Standard Normal Homogeneity (SNHT) and Pettitt and Buishand can be used.

3. Results

The calculation of the anomalies of the probability of rain and the average monthly precipitation allows us to infer how sensitive the study area is to the influence of the extreme phases of the ENSO phenomenon and to have a relative measure of the effect of these anomalies with respect to the average conditions. For example, if the anomalies are positive, this indicates an increase in the probability of rain and/or average monthly precipitation with respect to the historical average. If the anomalies are negative, this suggests a decrease in the probability of rain and/or average monthly precipitation. In the proposed methodology, the anomaly allows us to characterize the behaviour of the parameters analysed in each month of the year, without the need to have a complete historical series of data, inferring their monthly behaviour according to the ENSO phase.

3.1. Anomalies in rainfall probability

Anomalies in rainfall probability during the ENSO phase were calculated for each station using Equation 1, and then each station anomaly was calculated with Equation 4. Analysis of the historical data from each station shows that negative anomaly values in monthly rainfall probability prevail during El Niño phase. These anomalies represent approximately 63% of the total, and are particularly noticeable for stations 7037, 7067 and 7224, where such anomalies are seen for nine months of the year (see Figure 7). The only station where positive anomalies are observed for seven months of the year is station 7342, while for stations 7021 and 7119 the anomalies are seen for six months. In the rest of the stations, there are negative anomalies in various months of the year. The data was analysed to see whether there was any link between the positive or negative anomalies and the altitude of the stations, or their geographical location, but no correlation was found. However, it was observed that the stations with the highest number of positive anomalies in the rainy season (7007, 7021, 7037, 7054, 7145, 7180 and 7342) are in

the neighbouring basins 5, 6 and 7 (except for station 7007), in the southwest of the HSR (see Figure 2 and Figure 3).

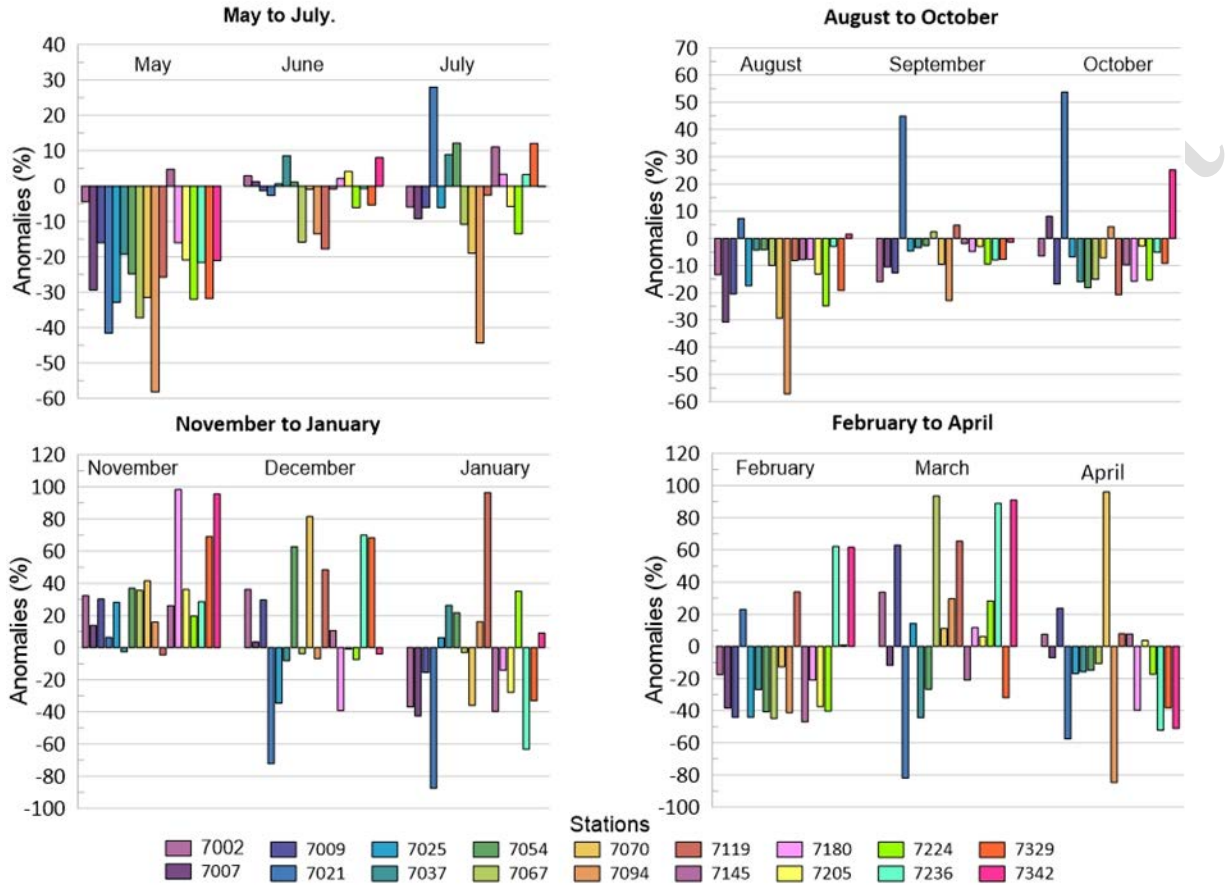

Figure 7 Anomalies in monthly rainfall probability during an El Niño phase

For a better visualisation of the results, the data were grouped in three-month periods, starting with May, the first month of the rainy season, and ending with April, so that the top two graphs show the rainy months, and the bottom panels the dry months.

In the La Niña phase, around 59.3% of months have positive anomalies in monthly rainfall probabilities, as seen in Figure 8. The data for stations 7007 and 7145 shows the greatest number of positive anomalies: 9 and 11 months of the year, respectively. Also, in the La Niña phase, in June and July (in the rainy season),15 of the 18 stations studied have positive anomalies, and in August all of them have positive anomalies. It is also worth noting that station 7021 has much greater positive anomalies than the rest of the stations from July to October. In contrast, at stations 7009, 7037, 7180 and 7236, negative anomalies prevail in more than 6 months of the year. For the other stations, positive anomalies are seen in different months. Once again, the analysis showed that there was no correlation between the values of positive or negative anomalies at stations with respect to altitude or geographical position.

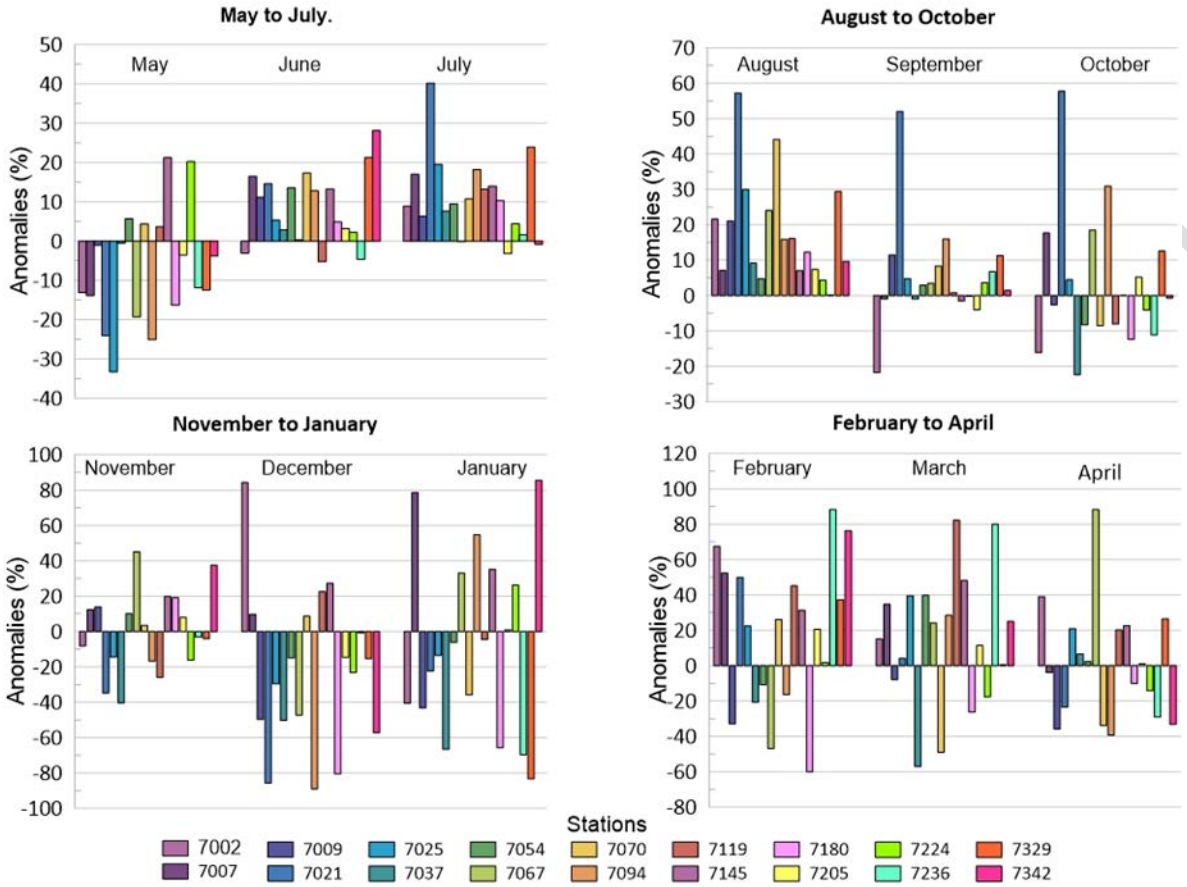

Figure 8 Anomalies in monthly rainfall probability during a La Niña phase

3.2. Anomalies in monthly mean precipitation

Monthly mean precipitation during the ENSO phase was calculated for each station, using Equation 3, and then each station anomaly was calculated with Equation 4. Figure 9 shows the monthly mean precipitation anomalies during the El Niño phase. The negative anomalies account for 56.5% of the total. From April to October, except for June, 66.6% or more of the stations have negative anomalies. Stations 7119, 7145 and 7329 are the only stations that have positive anomalies in more than six months, the rest have negative anomalies for six months or more. No correlation was found between the stations with the highest number of positive or negative anomalies regarding their geographical location or altitude.

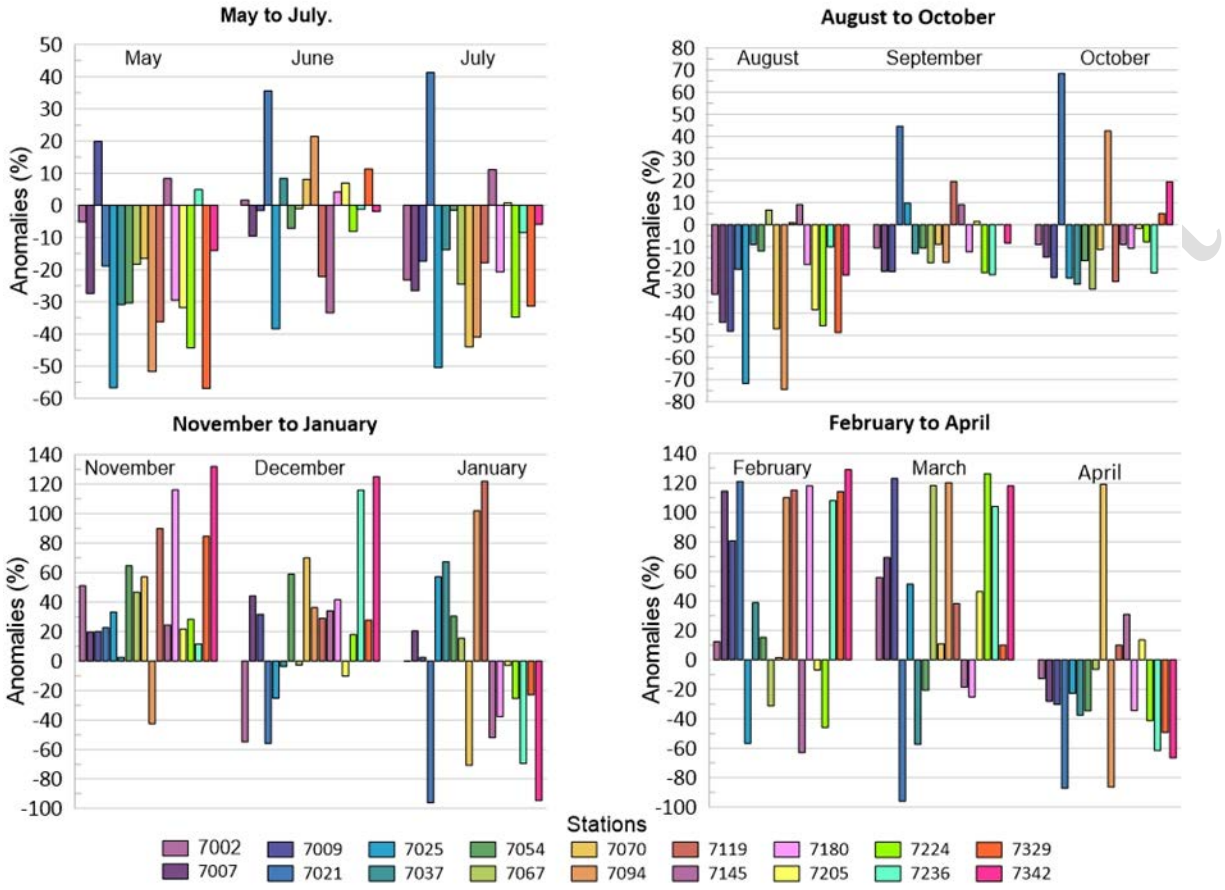

Figure 9 Monthly precipitation anomalies during an El Niño phase.

During the dry season, from November to April, monthly precipitation rates are very low, which explains why very large anomalies can be seen.

In Figure 10, the positive monthly precipitation anomalies during La Niña phase prevail with 57.9 % of the total. The months between June and September have the highest number of positive anomalies: over 70%. Stations 7002, 7025, 7070 and 7119 are the only stations that had negative anomalies in over six months, the rest had positive anomalies in six months or more. Station 7145 is the only station with positive anomalies in all months. It is worth noting that this station also had positive rainfall probability anomalies in eleven months of the year. In the La Niña phase, it is also worth noting that station 7021 had highest positive anomalies between July and October. No correlation was found between the stations with the highest number of positive or negative anomalies, with respect to their geographical location or altitude.

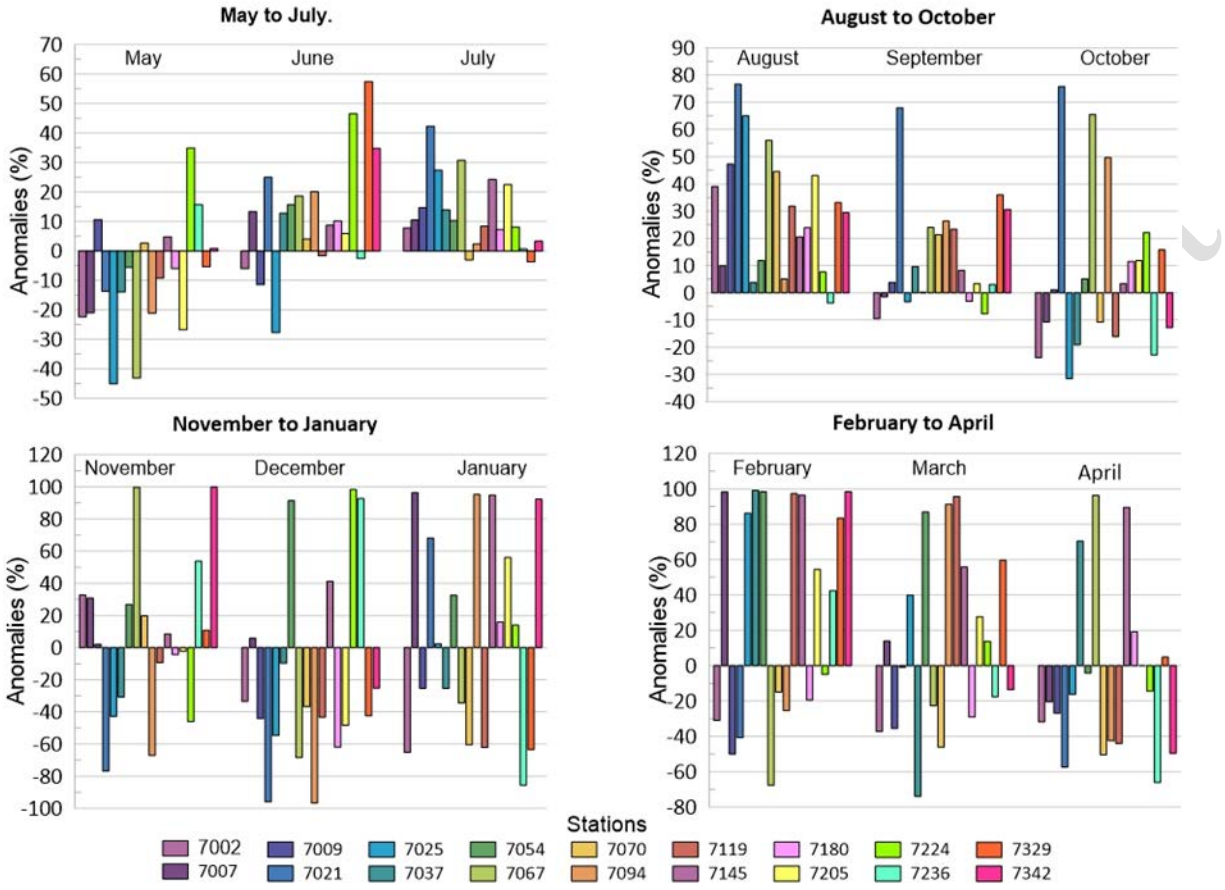

Figure 10 Monthly precipitation anomalies during a La Niña phase.

3.3. Volume total rainfall in the La Concordia HSR

Figure 11 shows the anomalies in the volume total rainfall for each station, which were found using the Thiessen Polygons and Kriging Spatial Interference methods. The anomaly values calculated with each method are quite similar in value and sign, except for the month of January for the El Niño phase, and November in the La Niña phase. It is seen that in the rainy season, except for the month of May, the volumes of precipitated water are greater in the La Niña phase: 20.0% higher than in the Neutral phase. The opposite is true when El Niño occurs: the volume of precipitated water is less with respect to the Neutral phase in the rainy season, with negative anomalies of over 20.0%. In the dry months, when rainfall is much lower, it is observed that in most months, except April, the anomalies are positive in El Niño phases, while in the La Niña phase, positive and negative anomalies are seen in the various months for the different stations.

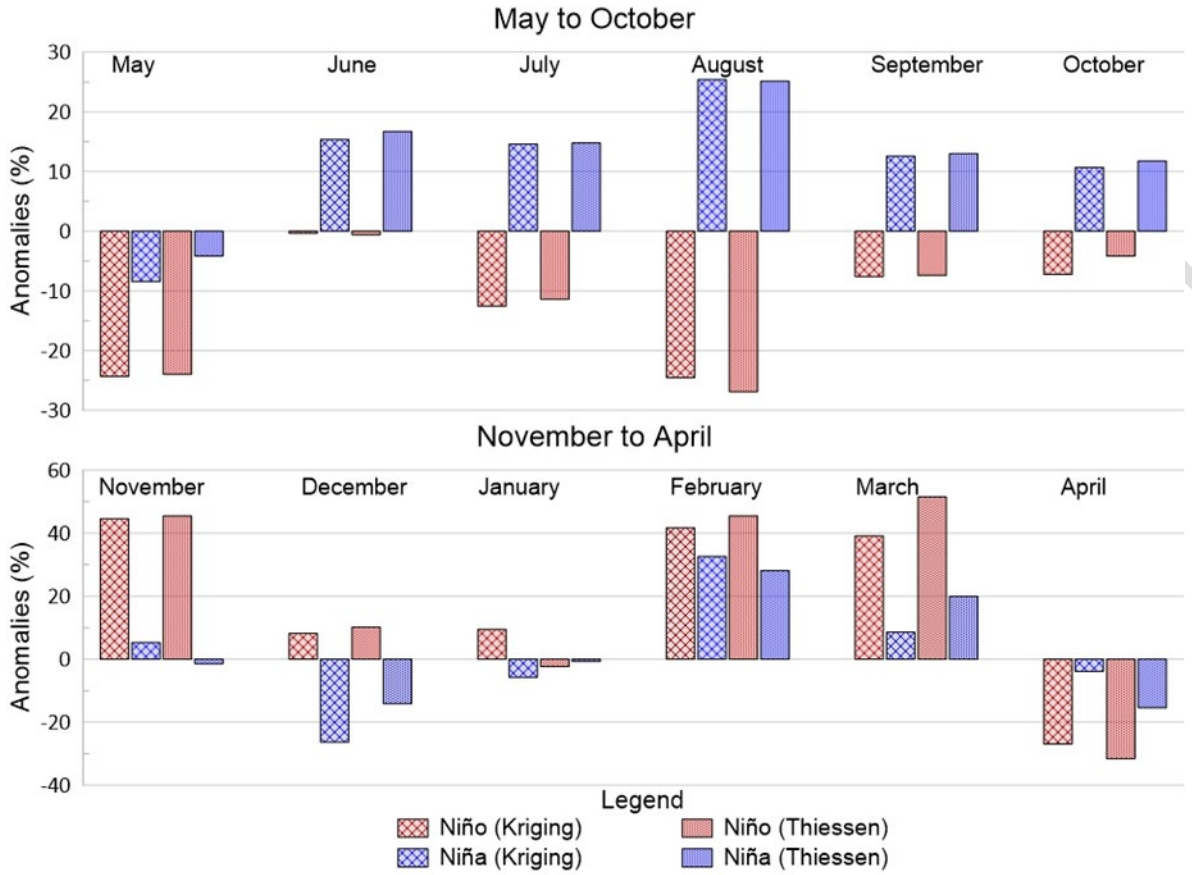

Figure 11. Anomaly values in monthly precipitation volumes in La Concordia HSR for the extreme phases of ENSO

4. Conclusions

The results obtained indicate that the different ENSO phases affect the rainfall patterns in the study area. In the rainy season, the El Niño phase has a negative effect on the probability of rainfall, as well as on the mean monthly precipitation, at over 60% of the stations studied. The opposite is observed for the La Niña phase, which positively affects the probability of rainfall and mean monthly precipitation, at over 57% of the stations in the rainy months.

Precipitation forecasts have become an essential tool in many fields; however, they still present a high degree of uncertainty due to the complexity of the physical mechanisms involved in the generation of precipitation [35]. From the results obtained, the following can be stated:

- The mean absolute percentage error obtained (MAPE) for the monthly rainfall forecast during the rainy months vary from 29% to 37% (Table 2), depending on the time series, which is considered a reasonable forecast [34]. However, for the dry months the MAPE obtained are considered inaccurate.
- In the case of the seasonal rainfall forecast, the MAPE values in the rainy season are less than 15%, which is considered a good forecast, and for the dry season these values vary between 27% and 38% (Table 3), which is considered a reasonable forecast [34].

Therefore, the proposed methodology works best for the calculation of seasonal mean precipitation, although reasonable monthly forecast values are obtained during the rainy months. This methodology does not work well in months when there is little rainfall.

As control and planning tools for urban and rural basins are gaining importance in water resource planning [36], the results obtained should be considered in future, more detailed studies, such as into the effect of ENSO phases in the various stages of the hydrological cycle (evaporation, infiltration, and runoff), and resultant availability of water for human consumption and hydroelectric generation. The results contribute to a better understanding of the climatology in the study area and ought to be taken into consideration in the future for decision-making during the planning of this precious resource.

Another relevant contribution of the work is the methodology presented, which allows the user monthly and seasonal forecasts of precipitation, as well as an analysis of these, in relation to ENSO phases. It is a reliable tool when analysis is required for an area where the historical records of daily precipitation data series are incomplete, as is the case of the study area.

In the future, we intend to examine how the extreme phases of ENSO affect the volume of surface water that runs into the reservoir of the La Angostura hydroelectric plant and analyse how this affects hydroelectric generation. This will also affect other downstream hydroelectric plants because insufficient rainfall means there will be less surface runoff, and in turn, less power can be generated. Indeed, very abundant rainfall may also affect hydroelectric generation, as the excess water in the reservoirs will have to be released. In addition, if the discharge of these excess volumes is not well managed, this could cause flooding downstream, affecting agricultural areas, and putting at risk downstream populations. Work on dam management in the study region such as that conducted by [37] for optimisation in a multi-dam system should be extended.

With this research, we hope that decision-makers in Mexico will be better equipped to undertake the technical management of reservoirs, particularly where continuous hydrological information is unavailable. We believe that this methodology is easily adaptable for the characterisation of the hydrological regime in other regions, particularly in developing countries where the historical information is often incomplete.

Declaration of competing interest

We declare that we have no significant competing interests including financial or non-financial, professional, or personal interests interfering with the full and objective presentation of the work described in this manuscript.

Acknowledgment

The authors would like to thank the Consejo Nacional de Humanidades, Ciencias y Tecnologías (CONAHCYT) for the support and financing of this research, which is part of the doctoral thesis of the author Maria-Felicia Jimenez-Lavie.

Funding

The Consejo Nacional de Humanidades, Ciencias y Tecnologías (CONAHCYT) provided a Scholarship to M.F. Jimenez-Lavie as a student of the Doctorate Program in Energy Engineering of the National Autonomous University of Mexico (UNAM).

Author contributions

All authors contributed to the study's conception and design. Maria Felicia Jimenez-Lavie: Material preparation, data collection and analysis were performed. José-Luis Lezama-Campos:

Statistical methods were proposed. Edgar Gerardo Mendoza-Baldwin and Rodolfo Silva-Casarín: Have contributed to the analysis and interpretation of results. Cecilia Martin-del-Campo: Research was conducted. Maria Felicia Jimenez- Lavie: The first draft of the manuscript was written and all authors participated to improve the present manuscript. All authors read and approved the final manuscript.

Data available statement

The authors confirm that the data supporting the findings of this study are available within the article [and/or] its supplementary materials.

References

[1] Iglesias Fernández I., Interacción Océano-atmosfera: Influencia de la SST y de la circulación termohalina. EPhysLab, Departamento de física aplicada, Universidade de Vigo, 2010.
[2] Groch, D.; Cogliati, M.; Finessi, F., Influencia de ENOS en la hidrometeorología de la Cuenca Alta del Río Neuquén, Geograficando, 16 (1), e066, 2020. [Online]. En Memoria Académica, Available: http://www.memoria.fahce.unlp.edu.ar/art_revistas/pr.11866/pr.11866.pdf, Accessed on: Oct. 8, 2022.
[3] Meteored, El cambio climático podría provocar "El Niño permanente", 2021. [Online]. Available: https://www.meteored.mx/noticias/ciencia/cambio-climatico-afectara-fenomeno-el-nino-ENOS-enos-ciencias-atmsofericas-oscilacion-del-sur.html. Accessed on: Oct. 16, 2022.
[4] Díaz-Esteban and Raga, G. B., Weather regimes associated with summer rainfall variability over southern Mexico, International Journal of Climatology, 38(1), 169-186, 2018. Available: https://doi.org/10.1002/ joc.5168
[5] IPCC, Informe de síntesis Contribución de los Grupos de trabajo I, II y III al Cuarto Informe de Evaluación del Grupo Intergubernamental de Expertos sobre el Cambio Climático [Equipo de redacción principal: Pachauri, R. K. y A. Reisinger (dirs. de la publicación)], IPCC, Ginebra, Suiza, 2007.
[6] NOAA, La Niña FAQs. National Ocean Service, 2017. [Online]. Available: https://www.pmel.noaa.gov/elnino/lanina-faq. Accessed on: Oct. 24, 2022.

[7] NOAA, Climate Variability: Oceanic Niño Index. National Ocean Service, 2009. [Online]. Available: https://www.climate.gov/news-features/understanding-climate/climate-variability-oceanic-ni%C3%B1o-index. Accessed on Oct. 20, 2022.

[8] Instituto del Mar del Perú (IMARPE), Índice Niño Oceánico (ONI), S.F. [Online]. Available: http://www.imarpe.gob.pe/imarpe/index2.php?id_seccion=I0178090500000000000000. Accessed on Oct. 20, 2022.

[9] NOAA, What are El Niño and La Niña?, National Ocean Service, 2021. [Online]. Available: https://oceanservice.noaa.gov/facts/ninonina.html. Accessed on: Oct. 27, 2022.

[10] Seneviratne, S.I., N. Nicholls, D. Easterling, C.M. Goodess, S. Kanae, J. Kossin, Y. Luo, J. Marengo, K. McInnes, M. Rahimi, M. Reichstein, A. Sorteberg, C. Vera, and X. Zhang., Changes in climate extremes and their impacts on the natural physical environment, In: Managing the Risks of Extreme Events and Disasters to Advance Climate Change Adaptation [Field, C.B., V. Barros, T.F. Stocker, D. Qin, D.J. Dokken, K.L. Ebi, M.D. Mastrandrea, K.J. Mach, G.-K. Plattner, S.K. Allen, M. Tignor, and P.M. Midgley (eds.)], A Special Report of Working Groups I and II of the Intergovernmental Panel on Climate Change (IPCC). Cambridge University Press, Cambridge, UK, and New York, NY, USA, pp. 109-230, 2012.

[11] Lopez, H., Lee, SK., Kim, D. et al. Projections of faster onset and slower decay of El Niño in the 21st century. Nat Commun 13, 1915, 2022. Available: https://doi.org/10.1038/s41467-022-29519-7

[12] NOAA, How will climate change El Niño and La Niña?, National Ocean Service, 2020. [Online]. Available: https://research.noaa.gov/article/ArtMID/587/ArticleID/2685/mediaid/2040. Accessed on: Oct. 27, 2022.

[13] NOAA, El Niño and La Niña: The El Niño Southern Oscillation (ENOS) is one of the most important climatic phenomena on Earth, National Ocean Service, 2015. [Online]. Available: https://www.noaa.gov/education/resource-collections/weather-atmosphere/el-nino. Accessed on: Oct. 27, 2022.

[14] Méndez González, J., Ramírez Leyva, A., Cornejo Oviedo, E., Zárate Lupercio, A. y Cavazos Pérez, T., Teleconexiones de la Oscilación Decadal del Pacífico (PDO) a la precipitación y temperatura en México, Investigaciones geográficas, (73), 57-70, 2010.

[15] Guevara-Polo D. and Mijares-Fajardo R, El Niño Oscilación del Sur (ENOS) y sus efectos sobre la precipitación en México. Entorno UDLAP, 15, 2021

[16] Comisión Nacional del Agua (CONAGUA), Atlas del Agua en México 2015, 2015. Available: http://www.conagua.gob.mx.

[17] Instituto Nacional de Ecología y Cambio Climático (INECC). La cuenca de los ríos Grijalva y Usumacinta, 2007. Available: http://www2.inecc.gob.mx/publicaciones2/libros/402/cuencas.html.

[18] Secretaria de Medio Ambiente y Recursos Naturales (SEMARNAT). (2015). Atlas digital geográfico. http://gisviewer.semarnat.gob.mx/aplicaciones/Atlas2015/agua_rios.html. Accessed 31 October 2022.

[19] Diario Oficial de la Federación (DOF), Acuerdo por el que se dan a conocer los estudios técnicos de aguas nacionales superficiales de las subregiones hidrológicas Alto Grijalva, Medio Grijalva y

Bajo Grijalva de la Región Hidrológica No. 30 Grijalva-Usumacinta. Secretaria de Gobernación, 29/04/2010.

[20] Instituto Mexicano de Tecnología del Agua (IMTA), Infraestructura Hidroeléctrica Actual. ISBN: 978-607-9368-93-7, 2017.

[21] Comisión Nacional del Agua (CONAGUA), Programa de Medidas Preventivas y de Mitigación de la sequía en el Consejo de Cuenca de los Ríos Grijalva y Usumacinta, 2014.

[22] Secretaria de Energía (SENER), Programa del desarrollo del Sistema Eléctrico Nacional (PRODESEN) 2018-2032, México, 2018.

[23] Comisión Nacional del Agua (CONAGUA), Estadísticas del Agua en México, edición 2010. Available: http://www.conagua.gob.mx.

[24] Instituto Nacional de Pesca y Acuacultura (INAPESCA), Capacidad de carga de la presa Belisario Domínguez (La Angostura). ISBN: 978-607-8274-26-0, 2021.

[25] Comisión Nacional del Agua (CONAGUA), Información de estación de Estaciones Climatológicas, 2019. [Online]. Available: https://smn.conagua.gob.mx/es/climatologia/informacion-climatologica/informacion-estadistica-climatologica, Accessed on: Oct. 30, 2019.

[26] Campos Aranda, D. F., Procesos del ciclo hidrológico. Facultada de Ingeniería. Universidad Autónoma de San Luis Potosí (UASLP), San Luis Potosí, S.L.P., México, 1998.

[27] NOAA, El Niño / Southern Oscillation (ENOS): Cold & Warm Episodes by Season, National Ocean Service 2021. [Online]. Available: https://origin.cpc.ncep.noaa.gov/products/analysis_monitoring/ensostuff/ONI_v5.php. Accessed on: May. 15, 2021

[28] NOAA, El Niño / FAQs. National Ocean Service, 2017. [Online]. Available: https://www.pmel.noaa.gov/elnino/faq. Accessed on: Oct. 18, 2022.

[29] NOAA, What is La Niña?, National Ocean Service, 2017. [Online]. Available: https://www.pmel.noaa.gov/elnino/what-is-la-nina. Accessed on: Oct. 27, 2022.

[30] Bedoya, M., Contreras, C., Ruiz., Capítulo 7: Alteraciones del régimen hidrológico y de la oferta hídrica por variabilidad y cambio climático. Estudio Nacional del Agua IDEAM, 2010.

[31] Sanchez Forero,N, Computation of average rainfall over la guajira pennisule using the Thiessen Method. Revista Ciencia e Ingenieria Neogranadina, Volumen 26(1): 97-108, 2016.

[32] Ponte Ramírez, Ricardo R. y Bosque Sendra, Joaquín, Comparación de Métodos de Cálculo Para la Obtención de la Variable Precipitación en un SIG. Estudios Geográficos, Vol 58 Num 226, 1997.

[33] Agua y SIG, Polígonos de Thiessen en ArcGis, 2011. [Online]. Available: https://aguaysig.com/poligonos-de-thiessen-en-arcgis/. Accessed on: Dec. 18, 2022.

[34] Lewis, C.D, Industrial and business forecasting methods. London: Butterworths, 1982.

[35] Arruti, Aldana, Ruiz, Juan, Salio, Paola, & García Skabar, Yanina, Evaluación preliminar de un sistema de pronóstico de precipitación a muy corto plazo basado en la extrapolación de datos sintéticos de radar, Meteorologica, 44(2), 56-77, 2019. Available: http://www.scielo.org.ar/scielo.php?script=sci_arttext&pid=S1850-468X2019000200004&lng=es&tlng=es.

[36] L. N.Garavito-Rincónet al., Revista Facultad de Ingeniería, Universidad de Antioquia, No. 113, pp. 106-113, 2024

[37] Mendoza-Ramírez, R.; Silva, R.; Domínguez-Mora, R.; Juan-Diego, E.; Carrizosa-Elizondo, E., Comparison of Two Convergence Criterion in the Optimization Process Using a Recursive Method in a Multi-Reservoir System. Water 2022, 14, 2952, 2022.